Development of a Novel Laser Polishing Strategy for Additively Manufactured AlSi10Mg Alloy Parts

Ben Mason[1[0000-0002-2136-3252]], Michael Ryan[1[0000-0002-8104-0121]], Rossi Setchi[1[0000-0002-7207-6544]], Abhishek Kundu[1[0000-0002-8714-4087]], Wayne Nishio Ayre[2[0000-0003-2405-1876]], and Debajyoti Bhaduri[1 [0000-0002-8270-388X]]

[1]School of Engineering, Cardiff University, Cardiff, CF24 3AA, UK
[2]School of Dentistry, Cardiff University, Cardiff, CF14 4XY, UK
MasonB4@cardiff.ac.uk

Abstract. Post-processing of additively manufactured (AM) aluminium alloy parts via laser polishing (LP) is particularly challenging due to the materials' high thermal conductivity, diffusivity, and reflectivity. Here, a novel multi-step laser polishing strategy, by combining laser ablation and smoothing steps, is developed that effectively reduces the surface roughness of AM AlSi10Mg parts. The minimum average roughness (Sa) and 10-point height (S10z) are achieved as 1.81 µm and 23.7 µm, representing maximum reductions of 94.1% and 89.8%, respectively, from the as-built AM surfaces (initial Sa 8 – 28 µm). A strong relationship has been observed between the initial surface roughness and the achievable roughness reduction. Regarding the other surface integrity factors, sub-surface microhardness (between 10-40 µm) after LP increases up to 182 $HV_{0.01}$, compared to the bulk hardness (105 $HV_{0.01}$) measured ~60 µm below the surface. Clear evidence of material's flow within the surface asperities during the LP steps is observed from the cross-sectional microstructures. Further study will involve in-depth analysis of materials' compositions within the LP-processed layers.

Keywords: Laser Polishing, Additive Manufacturing, AlSi10Mg Alloy.

1 Introduction

Additive Manufacturing (AM) offers immense benefits for design and manufacturing engineers, from the unparalleled geometric freedom afforded to unique material properties and potential for producing functionally-graded parts. Despite the reported advantages of AM technology over the conventional subtractive manufacturing methods, AM parts, especially metal parts, suffer from substandard surface roughness, requiring extensive post-processing before functional use [1]. There are a number of techniques available to modify the surface roughness of components, such as mechanical milling, grinding, electro-chemical polishing and so on, however these methods either suffer from reduced geometric freedom (in the case of milling) or cause environmental concerns (e.g., electrochemical polishing).

Laser Polishing (LP) is a promising alternative for the surface modification of AM parts. LP is a flexible, non-contact and automated method, only requiring line-of-sight between the optics and the surfaces to be processed, retaining much of the geometric freedom afforded by AM. LP also does not require any chemicals, and with a very low material removal the environmental concerns are also minimised.

2 Literature Review

2.1 AM Surfaces

It is well known that AM parts have much higher surface roughness values compared to the conventionally manufactured parts. A typical AM surface can have roughness values in the region of ~5-15 µm Ra, compared to milled surfaces, typically with ~0.5-6 µm Ra [2]. The high surface roughness of AM parts is detrimental to their functional properties such as tribological characteristics and fatigue resistance, as well as for their aesthetic appearance [3, 4]. These AM surfaces are dominated by tall peaks, deep valleys, adhered particles, and other surface contamination. While research has been undertaken to reduce the roughness by the AM parameters' optimisation [5, 6] the process is inherently limited in this regard due to the nature of the feedstocks limiting the possible resolutions and thus excess powder adhesion is common. Therefore, it is often necessary to post-process AM parts to reduce the surface roughness to an acceptable level.

2.2 Laser Polishing

Laser Polishing (LP), or more generally laser surface remelting, is the process of exposing a surface to laser irradiation to reduce the surface roughness. This occurs through melting of the surface material, which then flows by the effects of surface tension and capillary forces from high points (asperities) to low points (valleys). Due to the very high thermal gradients present in and around the melt pool (>10^3 K/mm [7]) the molten flow is highly turbulent, leaving a certain degree of residual roughness after each pass. When using a pulsed wave (PW) laser source, the residual surface texture also incorporates evidence of individual melt pools from the repeated melting and solidification as the bean traverses the surface.

With an excess energy input, a portion of the molten material vaporises and can be removed by extraction systems. This is known as ablation. Ablation results in a degree of material loss (~10 µm/pass) however at a much lower rate than would be expected by traditional machining processes (e.g., for milling, material loss is >500 µm/pass).

Both laser remelting and ablation processes are shown schematically in Fig. 1. One advantage of laser post-processing is the capability to incorporate surface functionalisation, such as adding textures to improve tribological performance [8] or corrosion resistance [9].

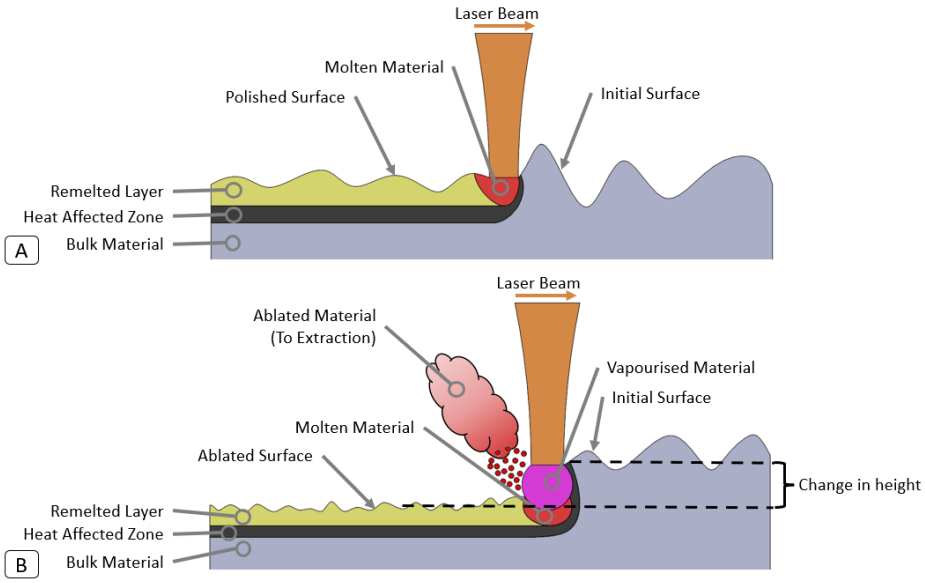

Fig. 1. Schematics of the (A) Laser Polishing and (B) Laser Ablation processes.

2.3 Laser Polishing of Aluminium Alloy Parts

Laser polishing has been implemented to post-process a varied range of metallic AM materials, such as stainless steel, titanium and nickel alloys over the past 20 years [10], however to a much-limited extent on aluminium-based alloys. This is because LP of aluminium alloy parts exhibits a particular challenge as the technology can be executed within a very narrow processing window. The high thermal conductivity (130-190 W/mK [11]) and high reflectance (>85% [12]) of Al alloys necessitate high energy inputs to heat the material, while the low melting point (~580 ºC) can result in over-heating of the parts. Furthermore, aluminium readily oxidises in air, and this oxide layer requires even more energy to melt.

So far, research into LP of AM aluminium has utilised both continuous wave [13], and nanosecond pulsed [14] laser systems. Despite the reported improvement in surface roughness following LP (~95%) it is difficult to draw conclusive remarks on the actual roughness reduction as either discrete LP locations were analysed for roughness measurement [13, 15] or different roughness filters were used for the polished and unpolished surfaces (0.8 mm and 0.25 mm respectively) [1, 16]. Since the quality of the AM surfaces vary greatly, it is essential to measure the same area before and after any surface treatment, where possible, and identical data processing operations applied.

The aim of this research is to develop a novel LP strategy that can effectively reduce the roughness of AM AlSi10Mg parts' surfaces. A multi-stage process is presented to combine ablation of large surface asperities, with remelting to remove smaller-scale features from the surface.

3 Methodology

3.1 Manufacture of the AM Specimens

The AM specimens were fabricated on a Renishaw AM250 laser-based powder bed fusion (L-PBF) system, using gas-atomised AlSi10Mg powder, also sourced from Renishaw plc. [11]. The manufacturing settings are recommended by the machine manufacturer for this particular Al alloy and are provided in Table 1, using the "meander" scan strategy. The samples measured 50 mm × 40 mm × 3 mm, with the 50 × 40 mm^2 surface built vertically onto an aluminium baseplate.

Table 1. AM samples' manufacturing settings.

AM parameters	**Values**
Laser Power	200 W
Hatch Spacing	100 µm
Point Distance	80 µm
Exposure Time	140 µs
Oxygen Content	<500 ppm

3.2 Laser Polishing

The 50 × 40 mm^2 surfaces (built vertically) were chosen for the laser polishing trials due to their higher surface roughnesses compared to the horizontally built surfaces. LP tests were conducted using a DMG Lasertec 40 laser milling centre, equipped with an SPI Lasers G3.1 laser source, the specifications of which are given in Table 2.

Table 2. Laser Specifications for SPI G3.1 module.

Laser machine specification	**Value**
Maximum Average Power	20 W
Laser Source	Yb-doped fiber laser
Focal Spot Diameter	32 µm
Beam Quality	$M^2 \approx 1.2$
Emission Wavelength	1064 nm
Pulse Frequency	≤ 290 kHz
Pulse Duration	15-220 ns (pre-set)

Two previous pieces of research were formative in the development of the LP methodology in the current research. The first by Bhaduri et al. [14], wherein the roughness reduction via a given LP strategy was improved by 80-88% when the samples were polished after placing them on a thermally insulating ceramic baseplate. It was surmised that the insulating baseplate reduced the conductive heat losses from the samples, reducing the cooling rates and in turn allowing the melt pools more time to re-flow before solidification. The researchers measured the sub-surface temperatures to be ~30% higher when using the baseplate compared to that recorded without the baseplate. Based on this, all trials in the present study were conducted with a thermally insulating ceramic baseplate between the samples and the laser machine's X-Y stage (made of stainless steel).

The second piece of work was by Petkov et al. [17] who proposed a multi-step strategy for LP of AM titanium alloy parts, comprising of steps designed to ablate the very tall peaks of the surfaces, followed by steps to remelt and smooth the surfaces. Previous unpublished work at Cardiff University developed an effective laser ablation strategy for AM AlSi10Mg samples, with laser pulse durations (T_e) of 15 ns, a pulse frequency (f) of 290 kHz, and fluence (F) of 14 J/cm^2.

Furthermore, in the work by Bhaduri et al. [14], the greatest smoothing effect for AM AlSi10Mg parts (~88% reduction in Sa after LP from the as-built surface) was found to be achieved with F = 12 J/cm^2, with pulse overlaps of 97% in both the X and Y directions. This was obtained using T_e = 220 ns and f =100 kHz.

Based on these, it was determined a multi-step process combining ablation and smoothing steps would maximise the potential for smoothing AM aluminium surfaces. The main thrust of this work involved iterating the speeds (v) and hatch spacings (h) for each step to determine the optimal pulse overlaps in the range of 90-97% in X and Y directions. This resulted in scan speeds between 275 and 925 mm/s for the ablation steps, and 100 to 300 mm/s for the smoothing steps. The hatch spacings were between 1 and 3 µm for all steps. Once the optimal pulses' overlaps were determined, the number of laser scanning passes for each step was also iterated between 2 and 20, with an increment of 2 passes from the previous iteration. Iterating the number of passes was done holistically, ensuring changes to one step did not necessitate changes to any other steps in the strategy. Finally, the focal offset settings were chosen such that the optimal fluence and pulses' overlaps were maintained at the maximum average laser power.

Throughout all the trials, the effectiveness of LP was evaluated based on the surface roughness response. The roughness response was chosen as this is the most widely assessed surface integrity factor and also due to the shorter analysis time compared to that required to analyse other surface/material properties. Once the final LP strategy was determined, further evaluations were conducted with respect to other surface integrity responses such as porosity, microhardness, and microstructure.

3.3 Surface Integrity Evaluation of the LP Specimens

Surface Roughness. The surface roughness of the samples was measured using a Sensofar Smart optical profilometer using the Focus Variation (FV) technique. FV essentially works by imaging a surface with a very narrow depth of focus at various distances. In each image, different regions are in focus; an algorithm then determines at which height each pixel is in the greatest focus [18]. The resulting pixel heights can then be displayed as a surface map or processed to determine various surface roughness parameters. Four standard roughness parameters were used in this work, namely arithmetic mean height (Sa), maximum peak height (Sp), maximum valley depth (Sv), and the ten-point height (S10z).

The surface roughness was initially measured on the unpolished surface and after each LP processing step to monitor the surface evolution through the strategy. Subsequently, only the initial and final surface roughnesses were measured. In all cases the surface measurements were post-processed using a 0.8 mm gaussian filter to isolate the roughness features.

Sub-surface Porosity. Once the final LP strategy was determined, a sample was laser polished according to the final strategy, sectioned, mounted, and mechanically polished using SiC papers, followed by diamond (6 and 3 µm) and silica (0.06 µm) suspensions.

Sub-surface porosity of the AM parts was estimated by direct observation on the cross-sections by using optical microscopy. A selection of the observed pores had the maximum dimensions measured, while the porosity was estimated using the ImageJ software to calculate the area coverage (%) from the surface to around 100 µm depth. Bulk porosity was estimated in a similar way, using optical micrographs from a central region.

Microhardness. Vickers microhardness measurements were conducted using a Mitutoyo MVK-G1 at a load of 0.01 kgf, and a dwell time of 10 seconds, in accordance with ASTM E92. Up to 50 µm depth below the LP surfaces, indents were spaced ~5 µm apart along the depth. Beyond this, the spacing was 10 µm to a final depth of 150 µm. Four indents were made at each depth at different locations. Indent diameters and depths below LP surfaces were measured using a Leica DM-LM optical microscope.

Microstructure. LP specimens were immersion etched in Keller's reagent (2.5% Nitric acid, 1.5% Hydrochloric acid, 1% Hydrofluoric acid) for 30 seconds to reveal the microstructure. Micrographs of the microstructure were then taken and inspected.

4 Results and Discussion

4.1 Surface Roughness

The optimum laser parameters of the developed LP strategy that rendered the minimum surface roughness values are listed in Table 3, while Fig. 2 displays how each LP step affected the roughness values with respect to the as-built surfaces. Figure 2 reveals that the first ablation step has the greatest influence on the Sa, Sp, and S10z values, while the final smoothing step causes the greatest reduction in Sv. Furthermore, only the Sp value is improved by the third step, clearly showing the ablation steps are effectively targeting surface asperities, while the smoothing step promotes material's filling in of the valleys. This exemplifies the benefit of the multi-step approach as the combination is far more effective than any one step in isolation when considering a range of roughness parameters.

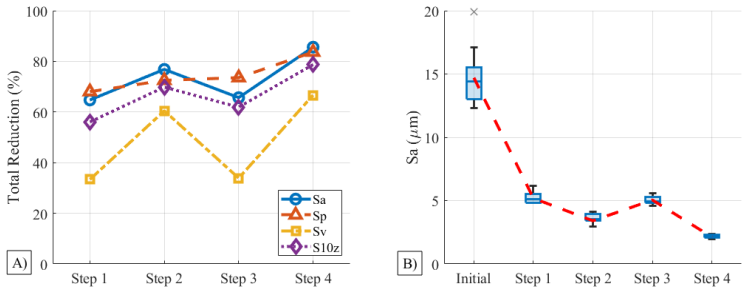

Fig. 2. (A) Total roughness reduction of various roughness parameters after each LP processing step and (B) measured Sa values after each LP step.

Figure 3 shows surface height maps and optical images of the same surface region in the as built state (A) and after each LP processing step (B-E). It is evident from the figure that the surfaces after the second and fourth steps (smoothing) are much smoother, with less variation in the heightmaps, and clear appearance. Fig. 3 C and E were taken with much lower illumination due to the increased reflectivity. The final surface shows no evidence of adhered particles or soot as is common on as-built AM surfaces.

Table 3. Settings for final LP strategy

LP Parameters	**Step 1** *Ablation*	**Step 2** *Smoothing*	**Step 3** *Ablation*	**Step 4** *Smoothing*
Scan Speed (mm/s)	620	325	620	325
Hatch Distance (µm)	3.3	3.7	3.3	3.7
Pulse Width (ns)	15	220	15	220
Pulse Frequency (kHz)	290	100	290	100
Focus Offset (mm)	-0.38	-1.34	-0.38	-1.34
Fluence (J/cm^2)	13.72	11.94	13.72	11.94
Pulse Overlap X (%)	94	95	94	95
Pulse Overlap Y (%)	91	94	91	94
Number of Passes	8	8	4	14

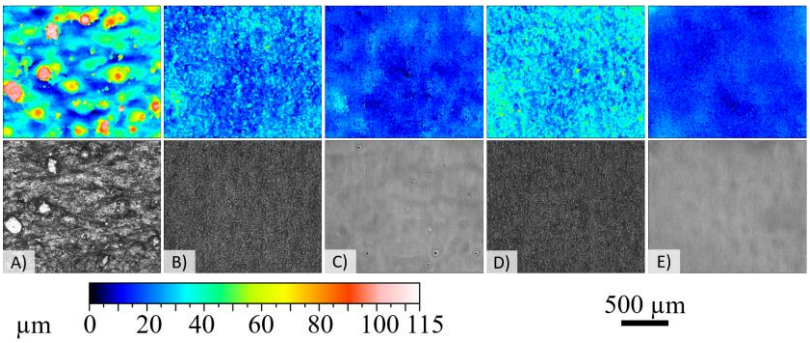

Fig. 3. Height maps (top) and optical images (bottom) of (A) the initial surface, and (B-E) after successive processing steps (Steps 1-4).

The minimum roughness values achieved with the developed LP strategy were 1.81 µm Sa, 12.8 µm Sp, 12.2 µm Sv, and 23.7 µm S10z. The corresponding maximum roughness reductions for each surface parameter were 94.1%, 91.6%, 83.5%, and 89.8% respectively. While evaluating the repeatability of the LP strategy in improving the surface finish it was noticed that the roughness reduction was lower at lower initial roughness values, as can be seen from Fig. 4. It has previously been reported by Hofele et al. [16] that their strategy was agnostic towards the initial surface roughness of parts. This was determined based on the average roughness values of surfaces built at various inclinations. Conversely, the present study shows that there is a relationship when considering the roughness of the same surface region before and after LP. Fig. 4 shows the roughness reduction data, along with an inferred trend and 95% confidence bounds for that trendline.

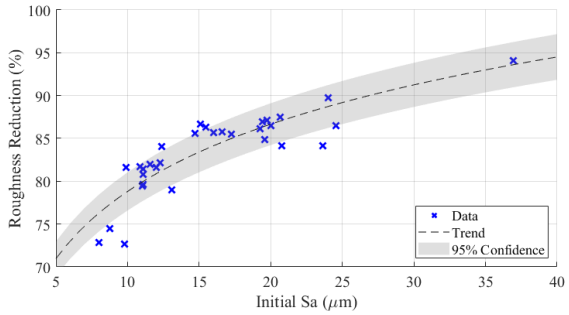

Fig. 4. Trend showing the relationship between the roughness reduction after LP and the initial roughness values.

4.2 Sub-Surface Porosity

From the cross-sectional micrographs (Fig. 5 (A)) it can be seen that there is an increase in the porosity concentration just below the melted layer (40-50 µm depth) after LP. This is possibly because the material flow during the smoothing step could not fully cover the ablated surface, trapping air beneath. The maximum dimensions of pores observed were 40 × 30 µm. Using the ImageJ image processing software, the porosity between the surface and 100 µm below the surface was estimated to be 5.8%, much higher than the 2.2% found in the bulk material.

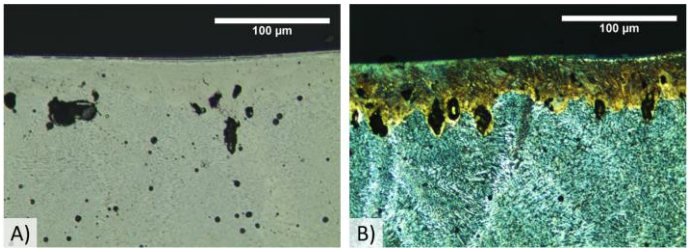

Fig. 5. Micrographs of (A) the surface region showing the sub-surface porosity, and (B) after etching to reveal the microstructure of the sub-surface region after the final LP step.

4.3 Microhardness

Figure 6 shows the microhardness data at various depths below the LP surface. It is observed that there is a slight increase in hardness beneath the LP surface (20% up to 10 µm depth) increasing to a maximum of 182 $HV_{0.01}$ between 30 and 40 µm depth. The bulk hardness of 105 $HV_{0.01}$ is achieved at depths greater than 50 µm. This is similar to findings by Bhaduri et al. [14] where surface hardening was observed following LP. The increase in the sub-surface hardness is possibly due to the enrichment of the silicon phases towards the surface [14]. However, unlike [14], no softer heat affected zone (HAZ) beneath the harder sub-surface layer is seen in the current study. Further investigations on the material compositions in the sub-surface layers after LP is under progress.

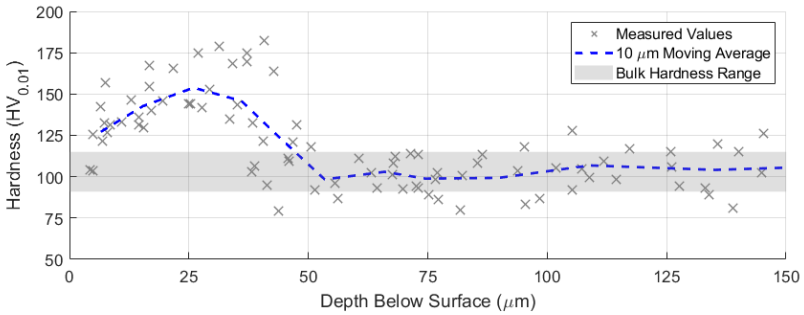

Fig. 6. Graph showing microhardness at different depths below the LP surface.

4.4 Microstructure

As described in section 2.2, one aim for LP is to reflow surface material from asperities into depressions to achieve a smoother surface. The evidence of this can be seen Fig. 5 (B) where the striations beneath the LP surface indicates successive layers of material have been deposited with each laser pass. Below this, a darker region exists, resulting from the proceeding ablation step (step 3). The unaffected region shows the typical fish-scale structures originated from the melt-pools of the L-PBF process.

5 Conclusions

The developed multi-step laser polishing strategy has proven to be effective at reducing the surface roughness (up to 94.1% reduction in Sa) of AM AlSi10Mg parts. The strategy combines ablation and smoothing steps to minimise the residual roughness by targeting different aspects of the surface parameters. Clear evidence of material redistribution is seen in the cross-sectional micrographs. A correlation between the initial surface roughness and roughness reduction due to LP is also revealed.

The LP strategy results in an increased hardness (up to 23% higher) between the surface and 60 µm depth (maxima at 40-50 µm) before bulk hardness is achieved. However, there is an increase in porosity concentration just below this hardened layer (5.8% compared to 2.2% in the bulk). This increased porosity is thought to be due to air being entrained in the surface after the ablation steps and trapped by the flowing molten material during the smoothing steps. The success of the developed LP strategy will be further implemented in large-scale post-processing of AM parts for functional applications in automotive and aerospace industry.

Acknowledgements

This research is supported by the EPSRC Doctoral Training Programme. Thanks are due to the Cardiff University's technical staff team during sample preparation. Special thanks are for Dr P. Penchev of the University of Birmingham and Prof R. Leach of the University of Nottingham for their valuable advice during the project. Special thanks must go to Dr F. Lacan for manufacturing the samples used throughout.

References

1. Hofele, M. et al.: Process parameter dependencies of continuous and pulsed laser modes on surface polishing of additive manufactured aluminium AlSi10Mg parts. Materwiss.

Werksttech. 52, 409–432 (2021). https://doi.org/10.1002/mawe.202000335.
2. Whitehouse, D.J.: Surfaces and their measurement. Kogan Page Science, London (2004).
3. Brandão, A.D. et al.: Fatigue Properties of Additively Manufactured AlSi10Mg-Surface Treatment Effect. Procedia Struct. Integr. 7, 58–66 (2017). https://doi.org/10.1016/j.prostr.2017.11.061.
4. du Plessis, A., Beretta, S.: Killer notches: The effect of as-built surface roughness on fatigue failure in AlSi10Mg produced by laser powder bed fusion. Addit. Manuf. 35, 101424 (2020). https://doi.org/10.1016/j.addma.2020.101424.
5. Calignano, F.: Investigation of the accuracy and roughness in the laser powder bed fusion process. Virtual Phys. Prototyp. 13, 97–104 (2018). https://doi.org/10.1080/17452759.2018.1426368.
6. Fox, J.C., Moylan, S.P., Lane, B.M.: Effect of Process Parameters on the Surface Roughness of Overhanging Structures in Laser Powder Bed Fusion Additive Manufacturing. Procedia CIRP. 45, 131–134 (2016). https://doi.org/10.1016/j.procir.2016.02.347.
7. Thijs, L., Kempen, K., Kruth, J.P., Van Humbeeck, J.: Fine-structured aluminium products with controllable texture by selective laser melting of pre-alloyed AlSi10Mg powder. Acta Mater. 61, 1809–1819 (2013). https://doi.org/10.1016/j.actamat.2012.11.052.
8. Wyatt, H., Elliott, M., Revill, P., Clarke, A.: The effect of engineered surface topography on the tribology of CFR-PEEK for novel hip implant materials. Biotribology. 7, 22–30 (2016). https://doi.org/10.1016/j.biotri.2016.08.001.
9. Xu, W.L., Yue, T.M., Man, H.C., Chan, C.P.: Laser surface melting of aluminium alloy 6013 for improving pitting corrosion fatigue resistance. Surf. Coatings Technol. 200, 5077–5086 (2006). https://doi.org/10.1016/j.surfcoat.2005.05.034.
10. Bhaduri, D. et al.: Laser polishing of 3D printed mesoscale components. Appl. Surf. Sci. 405, 29–46 (2017). https://doi.org/10.1016/j.apsusc.2017.01.211.
11. Renishaw plc.: AlSi10Mg-0403 powder for additive manufacturing, www.renishaw.com/additive, (2015).
12. Materion Microelectronics & Services: Reflectance in Thin Films. (2007).
13. Zhang, D. et al.: Investigation of laser polishing of four selective laser melting alloy samples. Appl. Sci. 10, (2020). https://doi.org/10.3390/app10030760.
14. Bhaduri, D. et al.: Pulsed laser polishing of selective laser melted aluminium alloy parts. Appl. Surf. Sci. 558, 149887 (2021). https://doi.org/10.1016/j.apsusc.2021.149887.
15. Zhou, J. et al.: In-situ Laser Polishing Additive Manufactured AlSi10Mg: Effect of Laser Polishing Strategy on Surface Morphology, Roughness and Microhardness. Materials (Basel). 14, 1–19 (2021). https://doi.org/10.3390/ma14020393.
16. Hofele, M. et al.: Laser Polishing of Laser Powder Bed Fusion AlSi10Mg Parts—Influence of Initial Surface Roughness on Achievable Surface Quality. Mater. Sci. Appl. 12, 15–41 (2021). https://doi.org/10.4236/msa.2021.121002.
17. Petkov, P. V, Penchev, P., Lacan, F., Bigot, S.: Finishing of Titanium ALM parts by Laser Ablation. In: WCMNM 2018 World Congress on Micro and Nano Manufacturing. pp. 111–114. Research Publishing Services, Singapore (2018). https://doi.org/10.3850/978-981-11-2728-1_85.
18. Danzl, R., Helmli, F., Scherer, S.: Focus variation - A robust technology for high resolution optical 3D surface metrology. Stroj. Vestnik/Journal Mech. Eng. 57, 245–256 (2011). https://doi.org/10.5545/sv-jme.2010.175.